PROCEEDINGS OF SCIENCE

Characterising the QGP with heavy flavour hadrons with ALICE: state of the art and prospects

Marianna Mazzilli for the ALICE Collaboration[a,*]

[a] *Wigner Research Centre for Physics and University of Houston*

E-mail: marianna.mazzilli@cern.ch

A transition to a phase of matter made of deconfined quarks and gluons, called the quark-gluon plasma (QGP), occurs in ultrarelativistic heavy-ion collisions. Heavy-flavour quarks (charm and beauty), because of their large mass, are mainly produced through hard scattering processes, on a shorter timescale with respect to the formation time of the QGP. Therefore, heavy quarks carry information about the different evolution aspects of heavy-ion collisions: initial conditions, QGP properties, hadronization mechanisms, and the rescattering in hadronic phase. In this contribution, a focus on the heavy-flavour measurements performed by the ALICE Collaboration that probe the properties and dynamics of the QGP is given. A summary on the state of the art of the characterisation of QGP properties with heavy-flavour hadrons and the prospects with ALICE upgrades are presented.

20th International Conference on B-Physics at Frontier Machines (Beauty2023)
3-7 July, 2023
Clermont-Ferrand, France

*Speaker

PoS(BEAUTY2023)040

1. Heavy-quark thermalisation and QGP transport properties

During the quark-gluon plasma (QGP) phase, the system exhibits a collective motion, which is governed by hydrodynamic principles. In particular, its constituents are subject to an outward boost, known as radial flow, which enhances their average transverse momentum (p_{T}). Furthermore, initial spatial anisotropies in the system lead to variations in the pressure gradients acting upon it, resulting in an azimuthally non-uniform momentum distribution of the outgoing partons, giving rise to an anisotropic flow [1]. The magnitude of this anisotropic flow can be quantified by the harmonic coefficients of the Fourier expansion of the final-state particle azimuthal-angle distribution, $\mathrm{d}N/\mathrm{d}\varphi$. The second harmonic, v_2, also known as elliptic flow, is the largest coefficient in non-central heavy-ion collisions. At low p_{T} ($p_{\mathrm{T}} < 10$ GeV/c), the v_2 of heavy-flavour hadrons provides information on the participation of charm and beauty quarks in the collective expansion of the medium [2] and on the fraction of heavy quarks hadronising via recombination with light quarks in the QGP medium [3, 4]. At high p_{T} ($p_{\mathrm{T}} > 10$ GeV/c), the v_2 of heavy-flavour hadrons can constrain the path-length dependence of energy loss in the medium. In Fig. 1, the elliptic flow v_2 of open charm

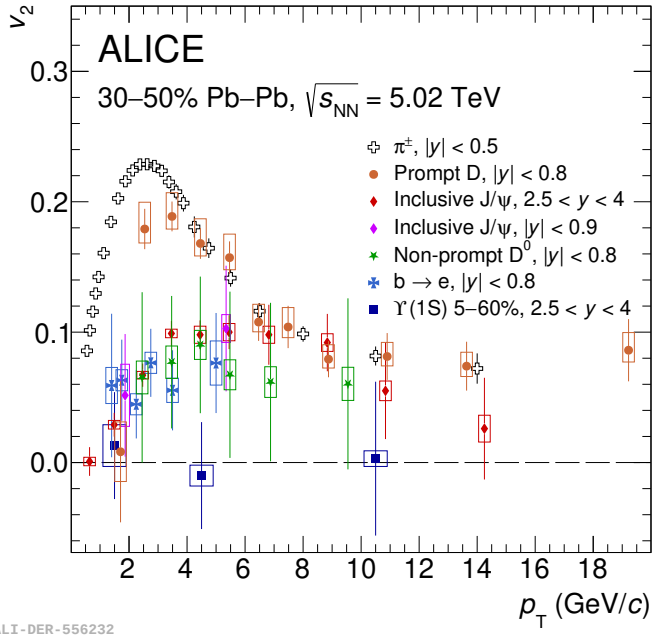

Figure 1: Elliptic flow v_2 of prompt D mesons [5] (orange markers), inclusive J/ψ at mid and forward rapidity [6] (magenta and red markers, respectively), non-prompt D^0 mesons [7] (green markers), beauty-decay electron hadrons [8] (light blue markers), bottomonium [9] (dark blue markers), and pions [10] (black markers) as a function of p_{T} in 30-50% Pb–Pb collisions at $\sqrt{s_{\mathrm{NN}}}$ = 5.02 TeV.

(average of prompt D^0, D^+ and D^{*+} mesons) [5], hidden charm (inclusive J/ψ) [6], D^0 mesons from beauty-hadron decays (non-prompt D^0 mesons) [7], electrons from beauty-hadron decays (b→e) [8], bottomonium (Υ) [9], and pions [10] is shown. A positive v_2 is observed for open charm and beauty hadrons and for inclusive J/ψ, while it is compatible with zero in the case of the bottomonium. In particular, the D-meson v_2 has a magnitude similar to the v_2 of charged pions in the interval $3 < p_{\mathrm{T}} < 6$ GeV/c, suggesting that low-p_{T} charm quarks have a relaxation time comparable to

the QGP lifetime and that the recombination of charm with light quarks from the medium plays a relevant role in the hadronisation. The non-prompt D^0-meson v_2, compatible within uncertainties with the v_2 of electrons from beauty-hadron decays, is lower (significance of 3.2σ) than that of prompt D mesons in $2 < p_T < 8$ GeV/c, indicating a lower degree of thermalisation of beauty quarks with respect to charm quarks.

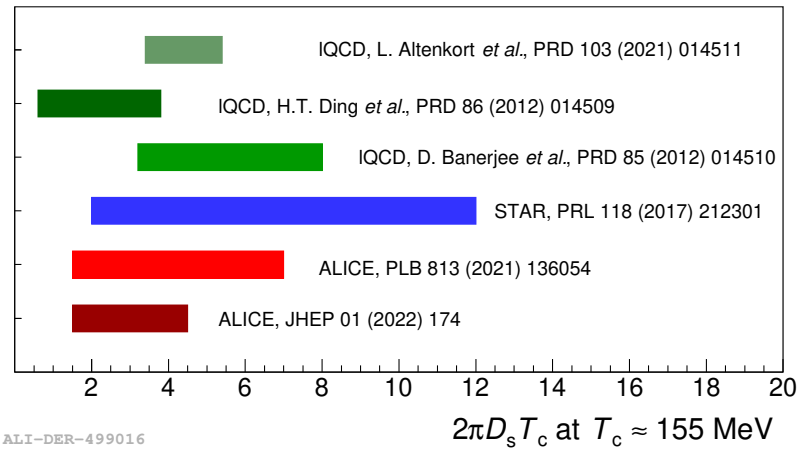

Figure 2: Spatial diffusion coefficient of charm quarks extrapolated from the model-to-data comparison of ALICE [5, 11] and STAR [12] measurements at the critical temperature T_c ≈155 MeV, compared to lattice QCD expectations [13–15].

The comparison of the open-charm hadron measurements with transport-model expectations [5] allowed for an estimation of the charm quark spatial-diffusion coefficient D_s which favours the range $1.5 < 2\pi D_s(T)T < 4.5$ at the critical temperature $T_c \approx 155$ MeV, as reported in Fig. 2. These values provide evidence that charm quarks couple strongly with the QGP at low momenta. The corresponding relaxation time ($\tau_{\rm charm} = \frac{m_c D_s}{T}$), $3 < \tau_{\rm charm} < 9$ fm/c, indicates that charm quark equilibration can occur during the QGP lifetime.

2. Energy loss in the QGP

Heavy-flavour quarks interact with the medium constituents via inelastic (gluon radiation) and elastic scattering that modify their momentum towards a thermal equilibrium with the surrounding quarks and gluons. As a consequence, high momentum charm and beauty quarks lose energy. The amount of energy loss is sensitive to the colour-charge dependence of the strong interaction, as well as to the effects that depend on the parton mass. In particular, beauty quarks are expected to lose less energy than charm quarks because of the "dead-cone" effect [16], which suppresses the gluon radiation of massive quarks at angles smaller than m_Q/E (with m_Q and E being the quark mass and energy, respectively) with respect to the quark direction.

The non-prompt-to-prompt D^0-meson nuclear modification factor (R_{AA}) ratio [17], presented in Fig. 3, is significantly larger than unity. Models that describe this ratio as a function of p_T encode a quark-mass dependence of energy loss and assume quark coalescence from the QGP, both effects being important as shown from the different modifications of LGR calculations [18] in the bottom panel of Fig. 3.

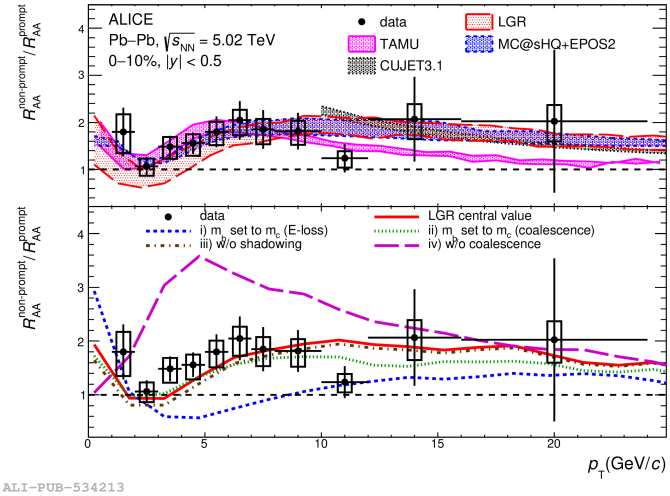

Figure 3: Non-prompt-to-prompt D^0-meson R_{AA} ratio as a function of p_T in the 10% most central Pb–Pb collisions at $\sqrt{s_{NN}}$ = 5.02 TeV [17], compared to model predictions (top) and to different modifications of LGR calculations [18] (bottom).

3. Prospect on QGP characterisation with ALICE upgrades

During the next data-taking period at the Large Hadron Collider, Run 4 (2029-2032), the ALICE heavy-flavour physics program will benefit from the improved resolution on the distance of closest approach deriving from the replacement of the three innermost layers of the current Inner Tracking System (ITS) with truly half-cylindrical layers (known as ITS 3) made of wide area ultrathin bent silicon sensors with a material budget reduced basically to that of the active silicon. Together with a new thinner and smaller beam-pipe this allows the placement of the first detection layer closer to the interaction point (from 22 to 18 mm). The combination of material reduction and the closer proximity of the inner layers to the interaction point improves the pointing resolution by a factor of about 2, as reported in the left panel of Fig. 4. As an example of the achievable physics performance, in the right panel of Fig. 4 [19] it is shown that the significance of the $\Xi_c^+ \rightarrow pK^-\pi^+$ improves by a factor of 4 with respect to ITS 2.

At the end of Run 4, there will still be open questions concerning the properties of the QGP phase, e.g. on the thermal equilibrium of heavy-flavour quarks, on the hadronisation mechanism in the QGP, and on the interactions of quarks and gluons within the QGP. A detector with unprecedented tracking capabilities will be necessary to address these physics topics with new measurements at the LHC [20]. The ALICE 3 detector concept extends the current R&D of ITS 3 project to a unique device for the measurement of heavy-ion collisions. The vertex detector will be located in a secondary vacuum within the beam-pipe, with the first layer positioned at 5 mm from the interaction point. Together with further silicon-based tracking layers this will provide a pointing resolution of 10 μm at p_T = 200 MeV/c. Particle identification will be possible over a broad momentum range thanks to Time-of-Flight stations at 19 and 85 cm accompanied by a Ring-Imaging-Cherenkov detector. The tracking and particle identification detectors will be housed in a superconducting magnet system. When operated at 2 T, a momentum resolution of 1% at η = 0 can be achieved. The unprecedented tracking and pointing resolution capabilities of the proposed detector, together

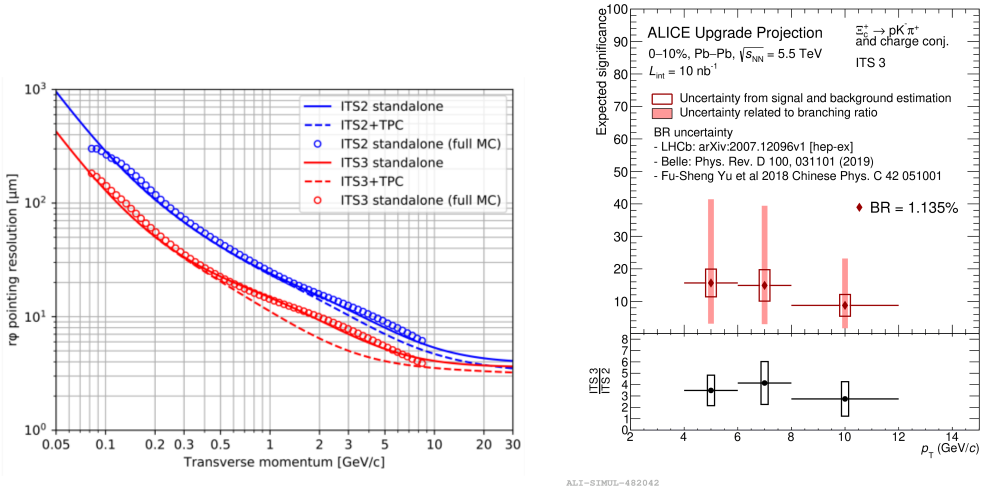

Figure 4: Left: comparison of pointing angle resolution as a function of the transverse momentum between ITS 2 and ITS 3. Right: expected significance of Ξ_c^+ reconstruction in 10% most central Pb–Pb collisions with ITS 3 (top) and ratio to the significance performance expected with ITS 2 (bottom).

with its large rapidity coverage ($|\eta| < 4$) and low p_{T} reach, will open a new era of measurements in the heavy-flavour sector. Performance estimates show that for the first time it will be possible to

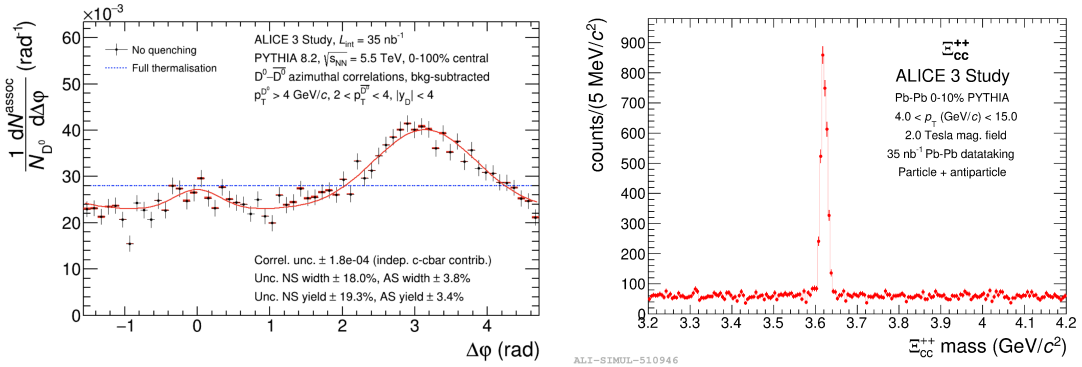

Figure 5: Left: expected performance for the measurement of the azimuthal distribution of $\mathrm{D^0\overline{D^0}}$ pairs in Pb–Pb collisions with the ALICE 3 detector. Right: expected invariant mass distribution for Ξ_{cc}^{++} candidates in Pb–Pb collisions with ALICE 3.

measure the azimuthal correlations of $\mathrm{D^0\overline{D^0}}$ pairs in Pb–Pb collisions. At low p_{T} this measurement probes the decorrelation in the QGP of charm and anti-charm quarks produced in pair in hard scatterings due to their interactions with the medium constituents and it is sensitive to the degree of thermalisation of the charm quark. An estimate of the performance with ALICE 3 is presented in the left panel of Fig. 5. Furthermore, the tracking layers at very small radii give the possibility to apply a new technique in the measurement of charged strange baryons, called "strangeness tracking", to directly track them together with their decay products identifying the clusters they produced in the vertex detector before the decay. The strangeness tracking will significantly boost the precision of measurements in the sector of multi-charm hadrons, since the prompt and non-prompt strange

hadrons can be separated. This will give access to measurements of multi-charm hadrons like the Ω_{cc}^{+} and Ξ_{cc}^{++}. An example of multi-charm hadron (Ξ_{cc}^{++}) invariant mass reconstruction with strangeness tracking is reported in the right panel of Fig. 5. Due to the early production of heavy-flavour quarks, the measurement of multi-charm baryons will give unique access to thermalisation and hadronisation mechanisms in the QGP.

References

[1] S. Voloshin and Y. Zhang, Z. Phys. C **70** (1996), 665-672 doi:10.1007/s002880050141

[2] S. Batsouli, S. Kelly, M. Gyulassy and J. L. Nagle, Phys. Lett. B **557** (2003), 26-32 doi:10.1016/S0370-2693(03)00175-8

[3] D. Molnar, J. Phys. G **31** (2005), S421-S428 doi:10.1088/0954-3899/31/4/052

[4] V. Greco, C. M. Ko and R. Rapp, Phys. Lett. B **595** (2004), 202-208 doi:10.1016/j.physletb.2004.06.064

[5] S. Acharya *et al.* [ALICE], JHEP **01** (2022), 174 doi:10.1007/JHEP01(2022)174

[6] S. Acharya *et al.* [ALICE], JHEP **10** (2020), 141 doi:10.1007/JHEP10(2020)141

[7] S. Acharya *et al.* [ALICE], [arXiv:2307.14084 [nucl-ex]].

[8] S. Acharya *et al.* [ALICE], Phys. Rev. Lett. **126** (2021) no.16, 162001 doi:10.1103/PhysRevLett.126.162001

[9] S. Acharya *et al.* [ALICE], Phys. Rev. Lett. **123** (2019) no.19, 192301 doi:10.1103/PhysRevLett.123.192301

[10] S. Acharya *et al.* [ALICE], JHEP **09** (2018), 006 doi:10.1007/JHEP09(2018)006

[11] S. Acharya *et al.* [ALICE], Phys. Lett. B **813** (2021), 136054 doi:10.1016/j.physletb.2020.136054

[12] L. Adamczyk *et al.* [STAR], Phys. Rev. Lett. **118** (2017) no.21, 212301 doi:10.1103/PhysRevLett.118.212301

[13] L. Altenkort, A. M. Eller, O. Kaczmarek, L. Mazur, G. D. Moore and H. T. Shu, Phys. Rev. D **103** (2021) no.1, 014511 doi:10.1103/PhysRevD.103.014511

[14] H. T. Ding, A. Francis, O. Kaczmarek, F. Karsch, H. Satz and W. Soeldner, Phys. Rev. D **86** (2012), 014509 doi:10.1103/PhysRevD.86.014509

[15] D. Banerjee, S. Datta, R. Gavai and P. Majumdar, Phys. Rev. D **85** (2012), 014510 doi:10.1103/PhysRevD.85.014510

[16] Y. L. Dokshitzer and D. E. Kharzeev, Phys. Lett. B **519** (2001), 199-206 doi:10.1016/S0370-2693(01)01130-3

[17] S. Acharya *et al.* [ALICE], JHEP **12** (2022), 126 doi:10.1007/JHEP12(2022)126

[18] S. Li, W. Xiong and R. Wan, Eur. Phys. J. C **80** (2020) no.12, 1113 doi:10.1140/epjc/s10052-020-08708-y

[19] S. Acharya *et al.* [ALICE], ALICE-PUBLIC-2023-002, https://cds.cern.ch/record/2868015

[20] S. Acharya *et al.* [ALICE], [arXiv:2211.02491 [physics.ins-det]]